

Crystal Structure of the Isotactic Alternate Copolymer between Carbon Monoxide and Styrene

Sergio Brückner*

*Dipartimento di Scienze e Tecnologie Chimiche, Università di Udine,
Via del Cottonificio 108, 33100 Udine, Italy*

Claudio De Rosa and Paolo Corradini

Dipartimento di Chimica, Università di Napoli, Via Mezzocannone 4, 80134 Napoli, Italy

William Porzio

Istituto di Chimica delle Macromolecole del CNR, Via Bassini 15, 20133 Milano, Italy

Alfredo Musco

Istituto di Scienze Chimiche, Università di Urbino, 61129 Urbino, Italy

Received July 21, 1995; Revised Manuscript Received October 19, 1995[§]

ABSTRACT: The crystal structure of a highly isotactic optically active alternating styrene–carbon monoxide copolymer, obtained with a chiral cationic Pd(II) bioxazoline complex, is determined and refined from powder X-ray diffraction data with the Rietveld method. The unit cell is monoclinic, $P2_1$ space group, with $a = 8.367$ Å, $b = 7.574$ Å (chain repeat), $c = 5.47$ Å, $\beta = 110.0^\circ$, and $Z = 2$ monomeric units with a density of 1.32 g/cm³. The observed chain conformation has a repeat period almost identical to that observed in syndiotactic copolymers in spite of the different symmetry connecting the monomeric units, $s(2/1)$ instead of tc . The different symmetry connecting the monomeric units along the chain influences significantly the reciprocal orientation of the phenyl groups within each chain and between different chains.

Introduction

Great interest is presently devoted to the study of the alternating copolymerization of α -olefins and carbon monoxide and to the possible stereospecificity of the polymerization reaction.^{1,2} Cationic Pd(II) 1,10-phenanthroline and 2,2'-bipyridine complexes catalyze the alternating copolymerization of styrene and carbon monoxide to a regioregular syndiotactic polymer.^{3–6}

With the above achiral ligands a chain end control of the polymerization is considered to be operative.⁷ It has been recently found by us and other authors that coordination of a chiral ligand to the metal switches the chain end control to yield isotactic optically active alternating copolymers.^{8–10}

Here we report on the structural characterization of isotactic poly(1-oxo-2-phenyltrimethylene) (hereafter i-STCO), a highly isotactic optically active alternating styrene–carbon monoxide copolymer obtained with a chiral cationic Pd(II) bioxazoline complex.

Recently, the structures of a series of syndiotactic copolymers of styrene^{7,11} and styrene derivatives¹² with carbon monoxide have been determined and some of them refined with the Rietveld method.¹³ It was therefore interesting to investigate the possible conformational differences involved by a configurational inversion on the tertiary carbon atom.

The need to study powder X-ray diffraction (XRD) data comes from the low molecular weight of the polymer that has not yet allowed us to obtain samples in the form of an oriented fiber. The Rietveld method,¹³ however, has already proved its validity in polymer crystallography, particularly when generalized coordinates are adopted to describe the model in order to

Table 1. Working Conditions for XRD Profile Recording

instrument	Siemens, D-500 goniometer equipped with step-scan attachment, Soller slit, and proportional counter
radiation (λ (Å), power)	1.5418 (Cu K α), Ni-filtered, 40 kV, 30 mA
divergence aperture (deg)	0.3
receiving aperture (deg)	0.05
angular range (deg, 2θ)	10–60
step width (deg, 2θ)	0.04
count time (sec per step)	70
temp	room

minimize the number of refinable structural parameters.^{12,14,15}

Experimental Section

i-STCO was prepared according to the procedure reported in ref 8. The powder X-ray diffraction profile of the crude polymer indicated a very poor crystallinity so that it was necessary to anneal the samples, and this was done either by suspending the polymer in octane or toluene at 80 or 100 °C under a N₂ flux or by stirring the dried powder in a heated vessel at 175, 200, or 220 °C for 1 h and then by cooling it to room temperature, cooling rate about 2 °C/min, under a N₂ flux.

DSC scans were carried out using a Perkin-Elmer DSC-2 instrument under a N₂ flux.

XRD profiles were recorded with a Siemens D-500 diffractometer under the conditions reported in Table 1.

The optical activity of the present samples was comparable to that reported in ref 8. The molecular weight, determined with a GPC analysis, was $M_w = 4900$ with a dispersity of 1.57 referred to polystyrene.

Thermal Behavior

The DSC trace (first scan) of a sample of i-STCO is reported in Figure 1. Two peaks are evident, the exotherm at about 448 K may be attributed to polymer

[§] Abstract published in *Advance ACS Abstracts*, January 1, 1996.

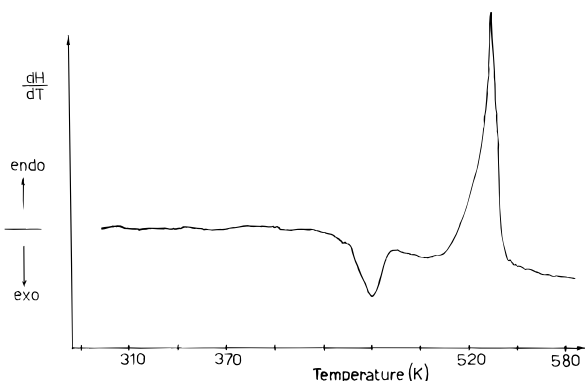


Figure 1. DSC trace of the first scan carried out on a sample of i-STCO.

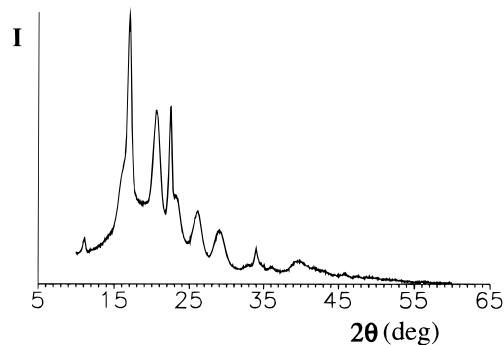


Figure 2. XRD profile of the sample annealed at 493 K and used for the Rietveld analysis.

crystallization, whereas the subsequent endotherm at about 526 K is due to polymer melting. In a second scan, however, no peak was detected, irrespective of the heating rate (from 2 to 20 K/min) and of the annealing time. This was ascribed to a severe decomposition that occurs during or after melting.

Annealing of the crude polymer significantly enhanced the degree of crystallinity only when carried out at temperatures higher than the crystallization peak (448 K). Several annealings were performed at 453, 473, and 493 K, higher temperatures being inadvisable due to incipient decomposition and to the observation that no further significant details arose in the XRD patterns of samples annealed at higher temperatures.

The XRD profile used for Rietveld analysis is that obtained from the sample annealed at 493 K and shown in Figure 2.

Structure Determination and Refinement

The "ab initio" structure determination from powder XRD data is a rather complex problem that only recently has been dealt with by Giovacazzo¹⁶ through an automatic procedure. In the case of polymer structures, however, the XRD profiles are usually of poor quality, characterized by a few peaks that, due to the relevant broadness, present many superpositions and quickly lose detectable intensity at increasing 2θ , so that 2θ ranges of only 60–70° are usually spanned to record significant data. The structure determination in this case is still a substantially "trial and error" procedure, which must treasure any available piece of information which is known a priori and allows for a significant reduction of the number of trials. The polymer chain repeat period and its internal symmetry are surely valuable hints for discriminating acceptable structural models. In the present case we started with the

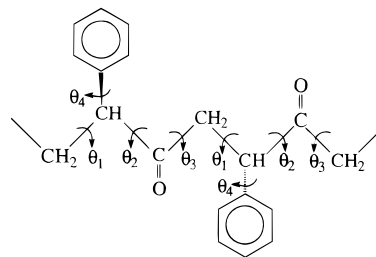


Figure 3. Definition of the dihedral angles refined in the structural analysis of i-STCO.

Table 2. Bond Lengths and Angles Used To Build the Model Monomer Unit of i-STCO and Kept Constant throughout the Refinement Procedure

bond lengths (Å)		bond angles (deg)	
C–C	1.53	C–C–C	111.0
C–C _{ar}	1.51	C _{ar} –C–C	111.0
C–C _{carbonyl}	1.51	C _{ar} –C _{ar} –C _{ar}	120.0
C _{carbonyl} –O	1.21	C–C _{ar} –C _{ar}	120.0
C _{ar} –C _{ar}	1.39	C–C _{carbonyl} –C	121.0

hypothesis that i-STCO presents a repeat period along the chain axis similar to that of the syndiotactic stereoisomer ($c = 7.5\text{--}7.6$ Å) whose structure has been already solved.^{7,11,12} This value would be consistent also with an isotactic chain configuration with the chain maintaining a nearly zigzag planar conformation and a $s(2/1)$ helical symmetry.

According to the equivalence principle¹⁷ a helical repetition $s(M/N)$ could occur in the case of an isotactic configuration, with a succession of internal rotation angles of the kind $\dots\theta_1\theta_2\theta_3\theta_1\theta_2\theta_3\dots$ (Figure 3). Highly extended chains ($c/M = 3.75\text{--}3.8$ Å) are obtained if θ_1 , θ_2 , and θ_3 are near 180°, that is $\theta_i = 180 + \delta_i$ with δ_i small. Let us assume (in accordance with qualitative energetic considerations) that bonds of opposite chirality (as defined in ref 17) adjoining a tertiary carbon atom along the chain have opposite deviations from the staggered conformations,^{17,18} if we assume $\theta_2 = -\theta_1$ exactly, then it is necessary that $\theta_3 = 180^\circ$ (for θ_1 near 180°) in order that the helix repeats after two monomeric units.

It may be seen that, in any case, for a 2-fold $s(2/1)$ helix conformation of a highly extended chain it must be $\delta_1 + \delta_2 + \delta_3 \approx 0$. For instance, for a chain with bond lengths and bond angles as in Table 2, if $\theta_1 = 165^\circ$ and $\theta_2 = -155^\circ$, then $\theta_3 = 170.3^\circ$ (with $\delta_1 = -15^\circ$, $\delta_2 = 25^\circ$, and $\delta_3 = -9.7^\circ$, i.e. $\delta_1 + \delta_2 + \delta_3 \approx 0$).

Slight deviations of the torsion angles of the main chain from the staggered conformation are feasible because of the low values of the barrier energy in the torsional potential energy around the bonds C–CO¹⁹ and suitable in order to relax nonbonded interactions between atoms appended to the chain.

The TREOR90²⁰ computing program was used to determine the unit cell. Some difficulty arose from the presence of peaks that, appearing as "shoulders" of other peaks, could not be precisely located on the 2θ scale. They also had to be included, however, in the starting set, being necessary for a correct indexing, and we decided therefore to lower the default value of the De Wolff figure of merit from 10 to 6 in order to make TREOR90 less selective. This increased the number of cells, giving a possible solution to the indexing problem; among them, however, a monoclinic primitive cell was selected that presents a number of features that are also satisfactory from the physical point of view.

Table 3. Crystal Data

repeat unit	C ₉ H ₈ O
fw	132.16
cryst syst	monoclinic
<i>a</i> (Å)	8.367(7)
<i>b</i> (Å)	7.574(4)
<i>c</i> (Å)	5.47(3)
β (deg)	110.0(1)
<i>V</i> (Å ³)	325.7
<i>Z</i>	2
space group	<i>P</i> 2 ₁
<i>d</i> _{calc} (g/cm ³)	1.347

Table 4. Bragg Angles (2 θ) and Bragg Distances (*d*) of the Reflections Observed in the X-ray Diffraction Spectrum of i-STCO of Figure 2.^a

2 θ (deg)	<i>d</i> (Å)	<i>d</i> _{calc} (Å)	<i>hkl</i>
11.2	7.90	7.865	100
16.3	5.44	5.454	110
17.0	5.22	5.188	101
20.6	4.31	4.281	111, 011
22.4	3.97	3.932	200
~23 ^b	~3.8	3.787	020
26.1	3.41	3.411	120
29.0	3.08	3.066	121, 021
32.9	2.72	2.727	220
34.0	2.64	2.621	300
36.0	2.49	2.477	310
39.6	2.28	2.270	131, 031
41.8	2.16	2.167	312

^a The calculated Bragg distances (*d*_{calc}) and the indices *hkl* are given for the unit cell of Table 2. ^b Shoulder.

First of all, it presents a *b* axis equal to the expected chain repeat period of ca. 7.6 Å; secondly, it indexes the observed peaks in agreement with their full widths at half-maximum (FWHM). In Figure 2 it may be in fact observed that the XRD profile contains peaks with different FWHM's. If we assume, as is usually the case, the lamellar thickness to be much smaller than the other two dimensions, we expect 0*kl* reflections (*b* coinciding with the chain axis) to be broader than *hkl* reflections, intermediate effects being expected for *hkl* reflections. A possible *P*2₁ space group was assumed considering the lack of 0*kl* peaks with *k* odd, the number of asymmetric units giving an acceptable density of 1.32 g cm⁻³ (within the range of densities detected in syndiotactic polymers¹²), and the necessary lack of any improper symmetry operation required by an optically active asymmetric unit. The 2-fold screw axis is also likely to describe the propagation of the polymer chain along the *b* direction, with the required repeat period, without involving a strained conformation. All these considerations led to a starting model for the refinement Rietveld procedure²¹ that was well-defined in its fundamental features. In Table 3 we report the crystal data of the present structure, and in Table 4 we list the indices *hkl* of the reflections observed in the spectrum of Figure 2. A monomeric unit was generated, according to the geometry reported in Table 2, and properly located on the 2₁ axis in order to give acceptable connections with the preceding and the following one, both generated by the screw axis. At this point, with the adoption of the rigid body model, the positions of all the atoms in the cell were only dependent on the rotation angle α of the whole monomeric unit around the 2₁ axis. This was the structural parameter that was refined first in order to get an initial rough-hewing of the model. The next step was to refine the molecular conformation with adjustment of the dihedral angles θ_i (*i* = 1–4) defined in Figure 3. In a way similar to that already adopted in the previous work on the

refinement of the structure of some derivatives of syndiotactic STCO¹² we refined the orientation of the asymmetric unit relative to the 2₁ axis, so that θ_1 , θ_2 , and θ_3 resulted simply by the symmetry relations connecting two successive monomer units, whereas θ_4 was defined within the asymmetric unit. At the beginning of the refinement θ_4 was kept fixed at –62° so that the phenyl plane bisects the valence bond at the tertiary carbon. Refinement of θ_1 , θ_2 , and θ_3 led to an improvement of the disagreement factor *R*₂' to 0.26,²² a value still high compared to other refined polymer structures. A significant lowering of *R*₂' to 0.133 was achieved by relaxing θ_4 , that changed to –96° with a significant tilt of the phenyls relative to the plane orthogonal to the chain axis. We were pleased to note that this conformational change is accompanied by a significant relaxation of intramolecular contacts between the oxygen atom and the close carbon atom of the phenyl ring. In fact this distance is lower than the sum of the Van der Waals radii (3.5 Å¹⁹) when the phenyl plane bisects the valence bond at the tertiary carbon (3.1 Å when θ_4 = –62°, 3.6 Å when θ_4 = –96°). In addition, some intermolecular contacts between phenyl rings of neighbor chains are also relaxed. These contacts did not go beyond 3.1 Å when θ_4 = –62°, whereas they are at 3.7–3.8 Å when θ_4 = –96°.

At this point we considered the possibility that folding effects at the lamellar surface may give rise to changes in the molecular direction, generating anticlinal chains, which, being not accounted for by the *P*2₁ symmetry, must be obtained through a noncrystallographic operation and are expected to substitute statistically the isoclined macromolecules. An anticlinal chain was then generated through a rotation of 180° around a noncrystallographic axis orthogonal to the chain axis and parallel to *c*.

This chain was allowed to translate along the *b* direction by a refinable shift relative to the original chain. An occupancy of one-half was attributed to all atoms. Refinement of this model produced a small reduction of the disagreement factor *R*₂' to 0.12 and showed a clear preference for the two chains to give a substantial overlapping of the phenyl rings. The reduction of *R*₂' is small as compared to the increase of the degrees of freedom of the refined model so that we are not inclined to assume, on the basis of pure crystallographic evidence, that this kind of directional disorder is really present in the polymeric crystals; it may only be argued that changes in the direction of the polymer chains are very likely to occur from a physical point of view and they are not excluded from our data.

Nonstructural parameters were refined as well. Crystallite dimensions along the three unit cell axes were optimized in order to reproduce the FWHM's of peaks, which are strongly dependent on the *hkl* triplets. A background line was evaluated through the contribution of a segmented line and that of a bell-shaped curve that approximately reproduces the X ray scattering from the amorphous phase. A small preferred orientation was refined along (010) together with a zero correction on the experimental 2 θ scale. Peak shapes were reproduced with Pearson VII functions with a refinable *m* parameter. The last refinement cycles were carried out with a total of 21 refinable parameters subjected to three geometrical restraints. Temperature factors were not refined.

In Figure 4 we show the comparison of the observed (a) with the calculated (b) XRD profiles; the background

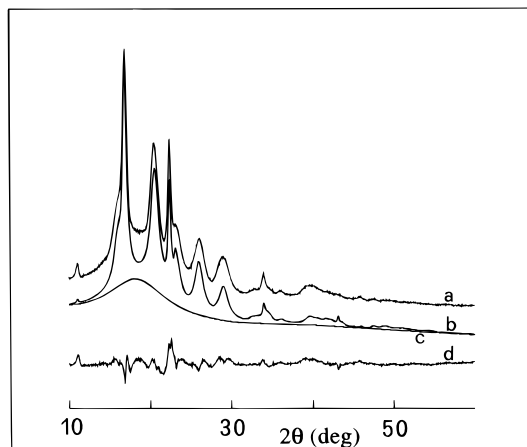


Figure 4. Comparison of the observed (a) with the calculated (b) XRD profiles. The background contribution is also shown (c) together with the difference profile (d).

Table 5. Refined Nonstructural Parameters

Zero Correction (deg, 2θ): 0.10(1)			
Profile Function Parameters (deg ²) ^a			
U	0	V	0.07(3)
W refined for each hkl triplet depending on the average crystallite dimensions			
Average Dimensions of the Crystallites along the Cell Axes (Å) ^b			
L_a	179(7)	L_b	23(1)
L_c	53(1)		
Pearson VII Exponent: $m = 1.01(5)$			
Preferred Orientation (rad ⁻²): ^c $G = 0.080(8)$ (along [010])			
Background Intensities (k Counts) ^d at the Nodes of the Segmented Line			
2θ (deg)	intensity	2θ (deg)	intensity
10	0.0480(10)	40	0.0230(2)
30	0.0249(5)	60	0.0068(2)
Isotropic Thermal Parameters B (Å ²) (Not Refined)			
O atoms	12	C atoms	6

^a Peak shapes calculated analytically with a Pearson VII function: $P = (C/H_k)[1 + 4(2^{1/m} - 1)z^2]^{-m}$ with $z = (2\theta_i - 2\theta_k)/H_k$ and $H_k^2 = U \tan^2 \theta_k + V \tan \theta_k + W$ where θ_k is the Bragg angle and W is different for each reflection and depends on the crystallite dimensions. ^b L_a , L_b , and L_c are affected by instrumental broadening; they are therefore only a rough underestimate of the actual average crystallite dimensions. ^c Preferred orientation is $PO = \exp(-G\alpha_k^2)$, α_k being the angle between the scattering vector of the k th reflection and the scattering vector of a fixed (preferred) orientation. ^d The background intensity was refined through the contribution of a segmented line with the superimposed bell-shaped curve having the form of a Pearson VII function with $m = 1.4$.

contribution is also shown (c) together with the difference profile (d). In Table 5 we list the values of nonstructural parameters that resulted from the refinement procedure.

Discussion of the Structure

In Table 6 the final fractional coordinates are listed. Bond lengths and angles were kept at standard values in the molecular building routine with the aid of geometrical restraints operating in the refinement cycles, so the only geometrical features subject to relatively free optimization were the torsion angles θ_i ($i = 1-4$). They are $\theta_1 = -161.5^\circ$, $\theta_2 = 155.3^\circ$, $\theta_3 = -171.4^\circ$, and $\theta_4 = -95.9^\circ$. We observe that θ_1 is similar to θ_2 but with opposite sign, in correspondence with the opposite chirality of the two bonds astride the tertiary carbon atom, and that θ_3 deviates by ca. 10° from the

Table 6. Fractional Coordinates

	x	y	z
C(1)	-0.0078(4)	-0.0022(1)	-0.0691(4)
C(2)	-0.070(2)	0.1753(3)	-0.002(2)
C(3)	-0.025(2)	-0.1712(3)	0.073(2)
C(4)	-0.258(1)	0.194(1)	-0.132(4)
C(5)	-0.324(1)	0.284(2)	-0.368(4)
C(6)	-0.499(1)	0.301(3)	-0.489(7)
C(7)	-0.609(1)	0.229(3)	-0.374(8)
C(8)	-0.544(2)	0.140(3)	-0.137(8)
C(9)	-0.369(2)	0.122(2)	-0.016(6)
O(10)	0.0550(9)	-0.0090(4)	-0.236(1)

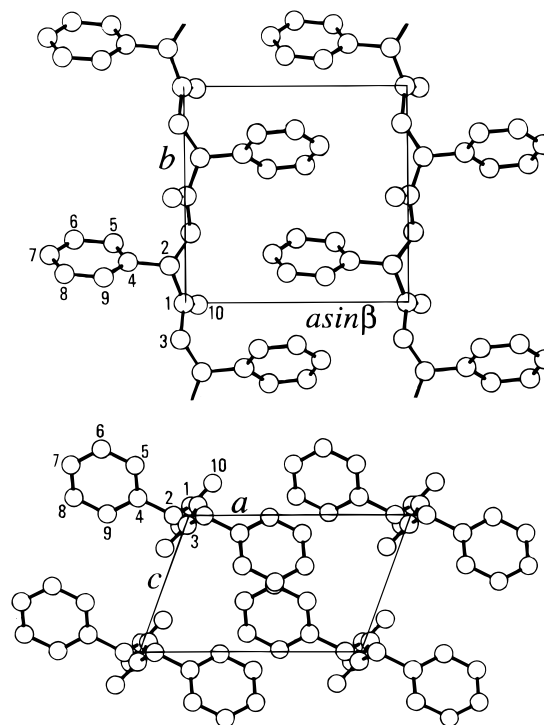


Figure 5. Refined packing model in b asin β and ac projections. The numbering scheme of the atoms belonging to a monomer unit is also shown.

trans conformation. These values resemble those refined in previous structural analyses on syndiotactic STCO¹¹ and other copolymers with various substituents on the phenyl ring;¹² it is of course important to note that a difference in the overall conformation is implied by the different symmetries that connect the monomer units along the polymer chain, i.e. *tc* in the syndiotactic polymers and *s(2/1)* in the isotactic polymer. The hypothesis that the configurational change at the tertiary carbons has no relevant effect on the chain repeat period is confirmed. A relevant difference concerns the value of θ_4 that, in this case, deviates significantly from -60° , the value that keeps the phenyl ring plane bisecting the valence bond at the tertiary carbon. This effect seems to arise from the need of optimizing intramolecular and intermolecular contacts and indicates the relative ease of rotation of the phenyls.

Intermolecular distances are all acceptable, the shortest C···C contacts being 3.7 Å, and this is true for both isoclined–isoclined and isoclined–anticlined chain contacts so that molecular packing is not expected to exert a discriminating effect toward the inversion of the chain direction. In Figure 5 we show the crystalline macromolecules viewed along b (the chain axis) and c ; the anticlined chains are omitted both for the sake of clarity and because their presence has not yet been proved with sufficient confidence. It is finally worthwhile to discuss

the refined average dimensions of the crystallites L_a , L_b , and L_c along the three cell edges reported in Table 5. In particular the low value of L_b (23 Å, lamellar thickness) is rather uncommon.

First of all, it must be pointed out that these parameters have not been corrected for instrumental broadening, and therefore they are only a rough underestimate of the real crystallite dimensions. However, even in the presence of large instrumental broadening effects, these dimensions are not likely to exceed 40–50 Å, a very small value, rather uncommon but not unique; in fact similar values (57 Å) have been found, for example, in polystyrene lamellae.²³ Secondly, we are not actually estimating the size of crystals but, more precisely, the size of coherently diffracting domains which, for example, do not include those parts of lamellar thickness involved in chain foldings. The polystyrene lamellae cited above would thus appear even thinner if their dimensions were evaluated through diffraction peak broadenings.

Acknowledgment. The authors thank Dr. S. V. Meille for helpful discussions. Financial support of the “Ministero dell’Università e della Ricerca Scientifica e Tecnologica” and of the “Consiglio Nazionale delle Ricerche” is gratefully acknowledged.

References and Notes

- (1) Sen, A. *Acc. Chem. Res.* **1993**, 26, 303.
- (2) Amevor, E.; Bronco, S.; Consiglio, G.; Di Benedetto, S. *Macromol. Symp.* **1995**, 89, 443.
- (3) Barasacchi, M.; Consiglio, G.; Medici, L.; Petrucci, G.; Suter, U. V. *Angew. Chem., Int. Ed. Engl.* **1991**, 30, 989.
- (4) Brookhart, M.; Rix, F. C.; De Simone, J. M.; Barborak, J. M. *J. Am. Chem. Soc.* **1992**, 114, 5894.
- (5) Sen, A.; Jiang, Z. *Macromolecules* **1993**, 26, 911.
- (6) Busico, V.; Corradini, P.; Landriani, L.; Trifuoggi, M. *Makromol. Chem., Rapid Commun.* **1993**, 14, 261.
- (7) Corradini, P.; De Rosa, C.; Panunzi, A.; Petrucci, G.; Pino, P. *Chimia* **1990**, 44, 52.
- (8) Bartolini, S.; Carfagna, C.; Musco, A. *Makromol. Chem., Rapid Commun.* **1995**, 16, 9.
- (9) Brookhart, M.; Wagner, M. I.; Bolavoine, G. G. A.; Haddon, H. A. *J. Am. Chem. Soc.* **1994**, 116, 3641.
- (10) Jiang, Z.; Adams, S. E.; Sen, A. *Macromolecules* **1994**, 27, 2694.
- (11) De Rosa, C.; Corradini, P. *Eur. Polym. J.* **1993**, 29, 163.
- (12) Trifuoggi, M.; DeRosa, C.; Auriemma, F.; Corradini, P.; Brückner, S. *Macromolecules* **1994**, 27, 3553.
- (13) Rietveld, H. M. *J. Appl. Crystallogr.* **1969**, 2, 65.
- (14) Immirzi, A. *Acta Crystallogr., Sect. B* **1980**, 2378.
- (15) Brückner, S. *Chim. Ind.* **1988**, 7/8, 48.
- (16) Altomare, A.; Cascarano, G.; Giacovazzo, C.; Guagliardi, A. *J. Appl. Crystallogr.* **1994**, 27, 435.
- (17) Corradini, P. In *The Stereochemistry of Macromolecules*; Ketley, A. C., Ed.; Marcel Dekker Inc.: New York, 1968; Vol. 3.
- (18) Corradini, P.; Pasquon, I. *Rend. Fis. Acc. Lincei* **1955**, 19, 453.
- (19) Napolitano, R.; Pirozzi, B. *Macromolecules* **1995**, 28, 2406.
- (20) Werner, P. E.; Eriksson, L.; Westdahl, M. *J. Appl. Crystallogr.* **1985**, 18, 367.
- (21) (a) Immirzi, A. *Acta Crystallogr., Sect. B* **1980**, B36, 2378.
(b) Millini, R.; Perego, G.; Brückner, S. *Mater. Sci. Forum* **1991**, 71–82, 239.
- (22) R_2' is defined as $R_2' = \sum |I_0 - I_c| / \sum I_{\text{net}}$, where I_{net} is given by $I_0 - I_{\text{backg}}$, so that the amorphous contribution, which is never negligible in polymer crystallography, does not artificially lower the disagreement factor.
- (23) Keith, H. D.; Vadimsky, P. G.; Padden, F. J., Jr. *J. Polym. Sci., Polym. Phys. Ed.* **1970**, 8, 1687.

MA9510505